Available online at ScienceDirect

Nuclear Engineering and Technology

journal homepage: www.elsevier.com/locate/net

Original Article

Building a Graphite Calorimetry System for the Dosimetry of Therapeutic X-ray Beams

*In Jung Kim**, *Byoung Chul Kim*, *Joong Hyun Kim*, *Jae-Pil Chung*, *Hyun Moon Kim*, *and Chul-Young Yi*

Korea Research Institute of Standards and Science, 267 Gajeong-ro, Yuseong-gu, Daejeon 34113, Republic of Korea

ARTICLE INFO

Article history:
Received 11 November 2016
Accepted 5 January 2017
Available online 11 February 2017

Keywords:
High Energy X-ray
Absorbed Dose
Graphite Calorimeter
Calorimetry

ABSTRACT

A graphite calorimetry system was built and tested under irradiation. The noise level of the temperature measurement system was approximately 0.08 mK (peak to peak). The temperature of the core part rose by approximately 8.6 mK at 800 MU (monitor unit) for 6-MV X-ray beams, and it increased as X-ray energy increased. The temperature rise showed less spread when it was normalized to the accumulated charge, as measured by an external monitoring chamber. The radiation energy absorbed by the core part was determined to have values of 0.798 J/μC, 0.389 J/μC, and 0.352 J/μC at 6 MV, 10 MV, and 18 MV, respectively. These values were so consistent among repeated runs that their coefficient of variance was less than 0.15%.

1. Introduction

Radiation therapy using high energy X-rays generated by medical linear accelerators has already been a major tool for cancer treatment. Approximately 30% of patients with cancer are undergoing radiation treatment [1], and 197 medical linear accelerators are currently operating in Korea [1–3]. Thus, radiation therapy quality control and assurance is very important for cancer treatment.

Radiation dosimetry is the most important indicator for quality control and assurance. When the irradiation is accurately performed at the prescribed dose, cancer cell death is maximized, whereas normal cell death is minimized. For this purpose, the International Commission on Radiation Units & Measurement recommends that the radiation dose measurement uncertainty should not exceed 5% [4].

The radiation therapy dose is calibrated in terms of the water absorbed dose (unit: Gy) [4–6]. The water absorbed dose is a physical quantity that is defined as the amount of radiation energy absorbed by water of a unit mass [4–6]. Water absorbed dose measurement can be realized with water calorimetry or by graphite calorimetry. Primary standard dosimetry laboratories use these types of calorimetry for primary dosimetry standards.

The world's first graphite calorimetry system was developed by S.R. Domen at the National Bureau of Standards in the 1970s [7]. Compared to water calorimetry, graphite introduces additional uncertainty owing to the necessity of converting the graphite absorbed dose to the water absorbed dose. However, the graphite method still has advantages over water calorimetry. One is that graphite has a specific heat capacity lower than that of water, which leads to a greater rise in

* *Corresponding author.*
E-mail address: kimij@kriss.re.kr (I.J. Kim).
http://dx.doi.org/10.1016/j.net.2017.01.015

temperature than is the case for water at the same absorbed dose. Another is that graphite has no thermal [8,9].

The sensitive volume or sensitive medium of a graphite calorimeter is called a core. Thermal isolation of the core from the environment is very important because the temperature at the core increases by only a few milliKelvins when a graphite calorimeter is irradiated by therapeutic X-rays. Thus, the core is usually covered with many layers of jackets in vacuum. In the core, there are one or more thermometers and heaters. The thermometer(s) is needed to measure the temperature rise of the core at irradiation. The heater(s) is needed for the calibration of the temperature rise to the energy absorbed in the core. The calibration is performed by comparing the temperature rise at irradiation to the temperature rise caused by known amounts of electric heat or energy. Thermistors, or resistive thermometers, are used for temperature measurements at the core as well as for heating. Thermistors have poor linearity and poor stability; however, they have sensitivity to temperature and are not affected by irradiation up to megaGrays [10]. In addition, thermistors are available in very small sizes, which is helpful for minimizing impurities in the core.

To ensure the repeatable measurement of the core temperature, the calorimeter must run under a quasi-adiabatic condition [11,12]. Under this condition, thermal transfer from the core to the inner jacket is kept nearly constant, and the temperature rise at the core is always proportional to the energy absorbed during its runs. A French group recently achieved this condition by introducing thermal feedback [13,14] to the inner jacket. In this study, a similar type of thermal feedback was developed and applied to achieve this quasi-adiabatic condition.

In this study, a graphite calorimetry system was built to measure the high energy X-ray absorbed dose. Experiments were performed to investigate system properties, and the results are discussed. In Section 4, the uncertainties of some values are given, but details are not provided as to how they were evaluated, because that is outside the scope of this article.

2. Materials and methods

2.1. Apparatus

2.1.1. Building graphite calorimeter

The graphite calorimeter (C1505-4) adopted a pan-shaped vacuum housing and double-layered jackets as in the design of the GR9 of the French group [13]. The core was covered with two layers of jackets and graphite mediums, and then placed in a vacuum housing and a graphite phantom. All of the graphite parts were composed of a batch product of high-density pyrolytic graphite (M507; Morgan Korea, Daegu, South Korea), whose density was separately determined to be (1.8154 ± 0.0014) g/cm^3.

The core was 16 mm in diameter and was 3 mm thick, with three sensing thermistors, one heating thermistor and three supports, as shown in Fig. 1. NTC-type thermistors with micro glass beads (diam.: 0.3 mm) were used (AB6B4-BR11KA103; GE Measurement & Control, U.S.A.). The thermistors had

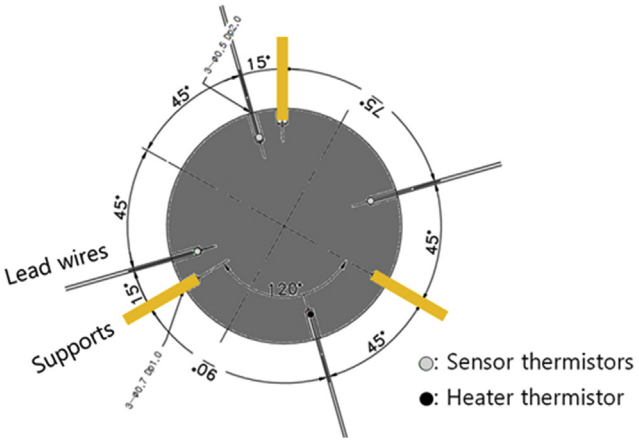

Fig. 1 – Schematic layout of the graphite calorimeter core (C1505-4).

resistances of 20 kΩ at room temperature; they contained nickel alloy lead wires (0.101 mm thick). Hollow Kapton tubes were used to support the core. Epoxy resin was used to glue all of the components of the core together. During the integration of the core, the core was weighed at each step to detect impurities (nongraphite ingredients). The jackets were prepared in the same manner as the core, but they were not weighed. The inner surfaces of the jackets were lined with thin aluminized Mylar foils to reduce radiative heat transfer. The outer jacket used a Manganin wire (LakeShore, OH, U.S.A.) (diam.: 0.202 mm) as a heater, instead of using thermistors.

After all parts were built, the thermistors were calibrated for temperature in a high precision water bath (7008, Fluke). The parts were separately placed in thin and watertight polyethylene bags (100 μm thick) and placed in the water bath. The temperature of the bath was measured using an SPRT (Standard Platinum Resistor Thermometer, 5187SA, Tinsley). The resistance of the thermistors and the SPRT was read using a high precision half-bridge (1595A, Fluke). Calibration was performed within a range of 20–30°C at each degree Celsius.

2.1.2. Electronics and external monitoring chambers

Wheatstone bridges were built to measure the temperature of the core and of the inner jacket. High precision standard resistors and decade resistors were used to build the bridges. A high precision voltage calibration source (3350A, Transmille) was used to supply the excitation voltage to the bridges. Nanovoltmeters (34420A; Agilent, CA, U.S.A.) were used to read the voltage difference across gaps in the bridges.

An electric heating and power measurement circuit was built, as shown in Fig. 2. In the figure, V_x represents the voltage drop across the heating thermistor of the core. R_s and V_s represent the resistance of a standard resistor and the voltage drop across the resistor, respectively. Then, the electric power dissipated at the heating thermistor, P_x, is given as $P_x = V_x V_s / R_s$. Electric power was fed by a multichannel dc power supply (2230-30-1, Keithley) to the heating thermistor. A precision resistor (SRL-10k; IET Labs., MA, U.S.A.) was used as the R_s; its

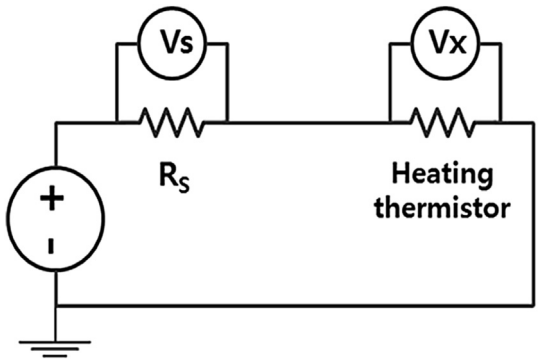

Fig. 2 – Diagram of a circuit for electric heating of the core and for measurement of electric power.

resistance was 9,999.2 ± 0.3 Ω. The voltage drop across the R_s and the heating thermistor was measured by two nanovoltmeters (34420A, Agilent), whose calibration coefficients were 1.00005 ± 0.00002 and 1.00001 ± 0.00002.

An external monitoring chamber system consisted of a set of two thimble-type ion chambers (0.53 cm^3) and a high precision electrometer. The chambers (Exradin A2, Standard Imaging) were held at 660 mm from the target, between the multileaf collimators and the calorimeter, and were separated by 125 mm in the cross-line direction. For the sake of buildup, the chambers were covered with high density pyrolytic graphite cylinders (inner diam.: 12.8 mm; outer dia.: 25 mm), and connected in parallel to the electrometer (6517B, Keithley). Bias voltage at −300 V was applied to the ion chambers. The room temperature and pressure were also measured to correct their effects on the ionization current measurement.

2.1.3. *Calorimeter operation and temperature analysis*

An operation platform was built using the LabVIEW program (National Instruments, TX, U.S.A.). The platform consisted of three modules. The first module read the temperature of the core and the inner jacket from the bridges, and used thermal feedback to control the temperature difference. The second module interfaced with the electric heating and power measurement circuit so that the circuit could control the electric power fed to the core and measure it. The third module interfaced with the external monitoring chamber system to read the accumulated electric charge of the ionizing current. Through the platform, all data points were acquired every 0.6 s. The temperature of the outer jacket was controlled separately using a standalone-type automatic temperature controller (350, Lakeshore).

A temperature analysis tool was coded using Mathematica 9.0.1. When it opened a file of the measured temperature data, it automatically found heating events (irradiation or electric heating) and analyzed the magnitude of the temperature rise. This tool used the interpolation function, provided by Mathematica 9.0.1, to enhance the capability of finding heating events. Heating events were easily recognized from the time derivative plot of interpolated points of the temperature data. The magnitude of the temperature rise was determined by linearly fitting the points, as shown in Fig. 3. The analysis was automatically performed, but required a manual input for initialization; this input was a roughly estimated value of the time width, that is, the period of events heating the calorimeter by electric power or irradiation.

2.2. *Experiments*

2.2.1. *Experimental set*

The calorimeter was mounted on a precision stage. The stage was moved so that the center of the core was placed 1,000 mm from the target of the accelerator; this accelerator was an Elekta Synergy Platform (Elekta, Stockholm, Sweden). The calorimeter was covered with graphite slabs, which made the mass thickness of graphite from the entrance of X-ray beams to the center of the core equal to approximately 10 g/cm^2. The mass thickness was separately determined to be (9.951 ± 0.008) g/cm^2.

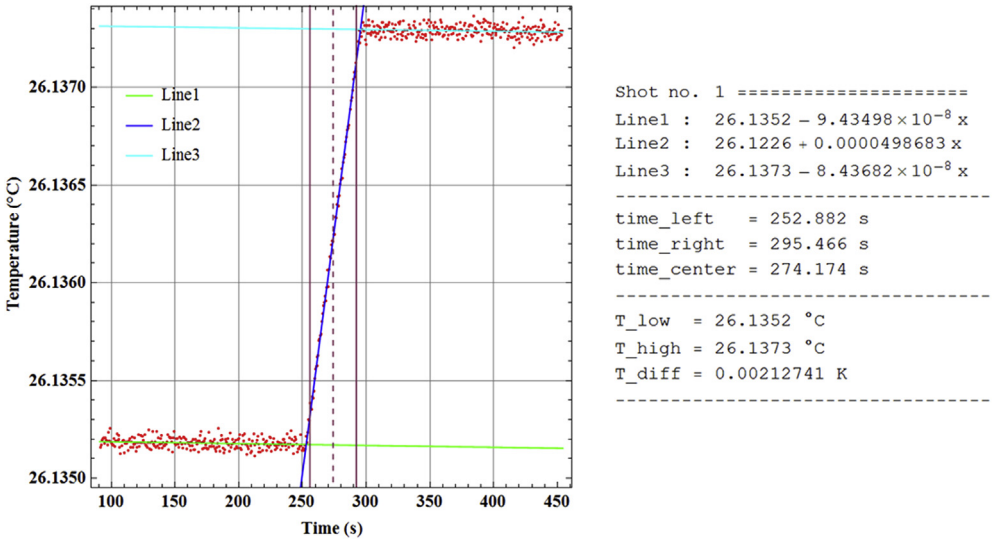

Fig. 3 – Temperature rise analysis at the core.

Table 1 – Measured mass of the core components (C1505-4).

	Value (g)	u_{std} (g)	u_{rel} (%)	Mass fraction
Graphite disk	1.098188	0.000006	0.0005	0.9952
Supports (Kapton)	0.000763	0.000002	0.20	0.0007
Thermistor beads	0.001748	0.000060	3.4	0.0016
Thermistor lead wires	0.001826	0.000086	4.7	0.0017
Glue (Epoxy)	0.000943	0.000002	0.17	0.0009
Total	1.10347	0.00011	0.0095	1

Table 2 – Estimation of heat capacity of the core (C1505-4) based on the measured mass of components.

	Specific heat		Heat capacity	
	Value (J/kg/K)	u_{std} (J/kg/K)	Value (J/K)	u_{std} (J/K)
Graphite [17] disk	706.9	0.6	0.7763	0.0007
Supports (Kapton) [18]	1,090	–	0.0008	–
Thermistor beads [17]	600	200	0.0010	0.0004
Thermistor lead wires [17]	900	200	0.0016	0.0004
Glue (Epoxy) [17]	1.800	300	0.0017	0.0003
Total		–	0.7815	0.0009

Table 3 – Results of thermistor temperature calibration.

	Parameters		
	A ($\times 10^{-6}$)	B ($\times 10^{-6}$)	C ($\times 10^{-9}$)
Core (C1505-4)	440 ± 11	247.9 ± 1.5	108.5 ± 4.0
Inner jacket	332.8 ± 7.8	253.9 ± 1.0	90.3 ± 2.7
Outer jacket	516.9 ± 1.0	253.38 ± 0.14	98.89 ± 0.42

Here, $T^{-1} = A + B \times \ln(R) + C \times (\ln(R))^3$,
where T is temperature given in K and R is resistance given in Ω.

The temperature of the outer jacket was maintained at 26°C. The Wheatstone bridges were activated at 0.8 V, and the heater thermistor of the inner jacket was also activated at 1.0 V to warm it up. When the temperatures of the core and the jackets were equilibrated, the temperature difference between the core and the inner jacket was set (at approximately 21 mK), and the thermal feedback was turned on. Then, the calorimeter was prepared for operation in the quasi-adiabatic mode.

2.2.2. *Electric heating and irradiation*

The calorimeter's response to the electric energy dissipation to the core was investigated. Electric energy was fed to the core for 140–172 s within a range of 6–8 mJ.

The calorimeter was irradiated at 800 monitor units (MU) using 6-MV, 10-MV, and 18-MV X-rays at 300 MU/min, 410 MU/min, and 350 MU/min, respectively. It took approximately 140–172 s to complete an irradiation of 800 MU for each X-ray beam. Prior to or between every irradiation, electric heat was also provided to the core to compare the core's response to irradiation and to electric heating

3. Results and discussion

The measured mass values of the core components are shown in Table 1. The total mass values of the core and its impurities were 1.10347 ± 0.00011 g and 0.00528 ± 0.00011 g, respectively. Thus, the portion of the core that consisted of impurities was 0.48%, which was as good as the number reported by the French group (GR-09, 0.59%; GR-10, 0.90%; GR-11, 0.35%) [14,15] or by the Japanese group (1.5%) [16]. Based on the measured mass of the core components, the heat capacity of the core was expected to be as shown in Table 2. According to the

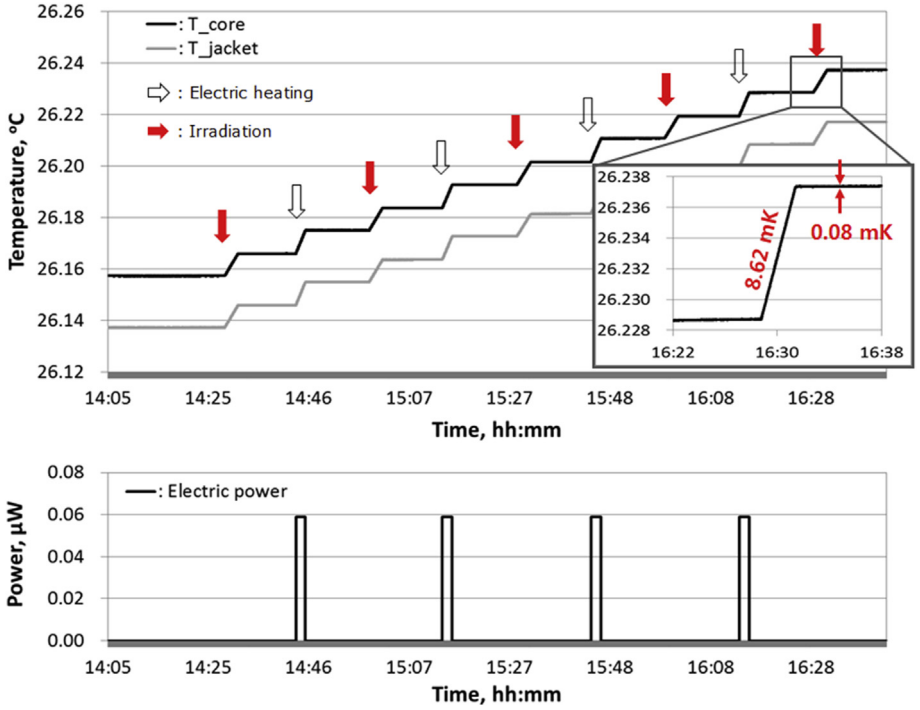

Fig. 4 – Measured temperature change of the core (T_core) and the inner jacket (T_jac).

measured mass and the known values of specific heat, the core heat capacity was estimated to be 0.7815 ± 0.0009 J/K.

Thermistors were calibrated to temperature by applying the Stein–Hart model equation [19], as shown in Table 3. The uncertainty of the fitting parameters for the core was slightly large. According to the error propagation equation, the uncertainty of the temperature rise by 10 mK at 26°C was expected to be 0.9%. Furthermore, it is known that Wheatstone bridges with DC excitation voltage are not very stable [16], which means that the uncertainty of the absolute value of the temperature rise will be larger than 0.9%.

The temperature of the core and the inner jacket rose, as shown in Fig. 4, under irradiation and electric heating. The noise level at the Wheatstone bridge was about 0.3 μVpp (peak to peak), which corresponded to approximately 0.08 mK in temperature. The core temperature rose by approximately 8.6 mK at 800 MU for 6-MV X-ray beams; core temperature increased as X-ray energy increased. It was possible to very accurately measure the electric power dissipated in the core ($u_{std} = 0.015\%$) because of the small uncertainties of the resistance and of the voltmeters. However, owing to the poor time resolution of the data sampling (0.6 s), it was expected that the amount of electric energy dissipated might have a larger spread. Assuming a uniform distribution, uncertainty of time might be 0.35 ($=0.6/\sqrt{3}$) s, which would cause the determined electric energy to spread by 0.2%.

The calorimeter's response to the electric energy dissipation at the core is shown in Fig. 5. It was very linear, within 6–8 mJ ($R^2 = 0.9997$), with a slope of 1.242 ± 0.003 K/J. The inverse of the slope (0.805 J/K) corresponded to the effective heat capacity of the core, but it was larger by 3% than the heat capacity, which was expected according to the data shown in Table 2. This discrepancy might be attributable to the uncertainty of the temperature measurement (>0.9%), the ambiguity of the cited specific heat values or thermal loss from the core to the inner jacket.

The intercept (0.056 mK) of the fit was not ignorable compared with its uncertainty (0.023 mK), but it was sufficiently small compared with the noise level (0.08 mK). Thus, it was determined that the intercept could be ignored for the calibration of the temperature rise to the energy absorbed in the core. So, the effective heat capacity of the core was obtained at every run as the ratio of electric energy dissipation to the temperature rise. The coefficient of variance of the effective heat capacity was approximately 0.2%, which was mainly attributable to the uncertainty of the determination of the electric energy dissipated in the core.

Under irradiation, the temperature rise of the core showed good correlation with the accumulated charge of the external

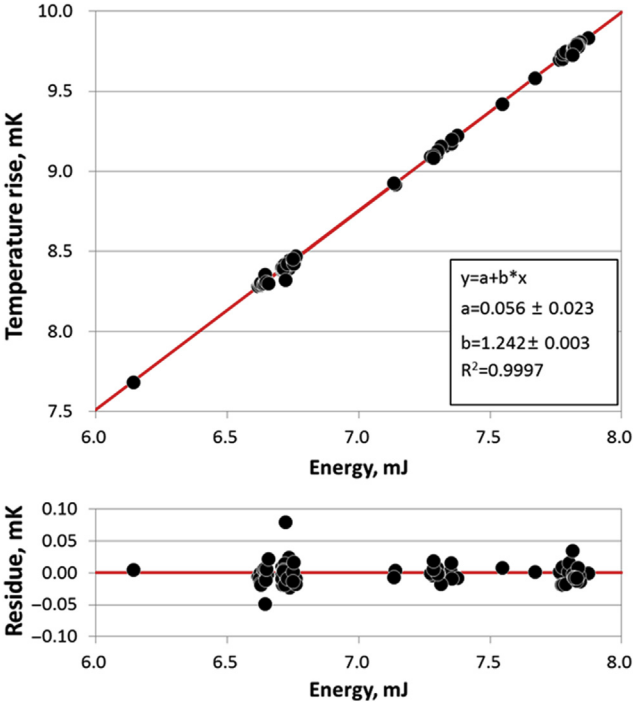

Fig. 5 – Plot of core temperature rise according to electric energy dissipation.

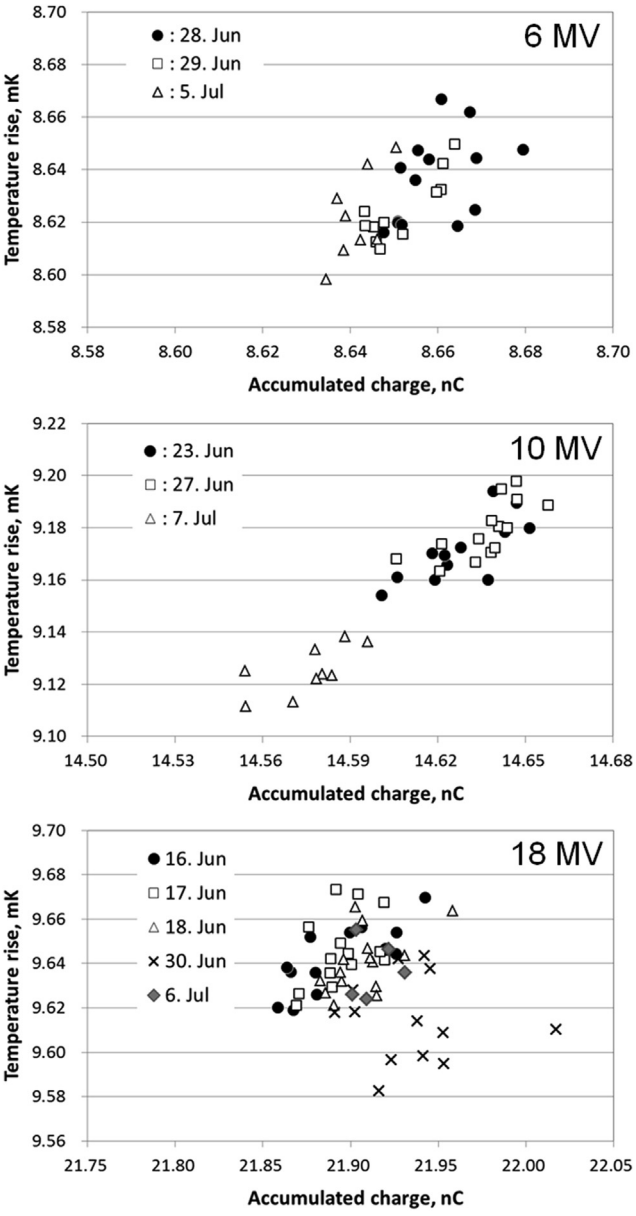

Fig. 6 – Correlation between temperature rise of the core and accumulated charged of the external monitor chamber at 6-, 10-, 18-MV X-ray beams.

monitoring chamber. If the internal monitoring chamber of the accelerator had been sufficiently accurate to monitor the X-ray beams, the temperature rise of the core should have shown no correlation with the accumulated charge of the external monitoring chamber, because all irradiation was performed at 800 MU. However, the measured temperature rise showed obvious correlations for the 6-MV and 10-MV X-ray beams, as shown in Fig. 6. Even at 18 MV, the data points, except those measured on June 30, 2016 still showed good correlation. The reason for the anomaly that surfaced on June 30 is not understood yet, but will be further investigated. In any case, the overall correlation coefficients at 6 MV, 10 MV, and 18 MV (excepting the abnormal data points) were 0.64, 0.94, and 0.47, respectively. Thus, it was convincingly demonstrated that, to achieve better data, the temperature rise of the core should be normalized to the accumulated charge of the external monitoring chamber. Also, the coefficients of variance of the temperature rise were around 0.2% or 0.3%, but dropped by approximately 0.1% when they were normalized to the accumulated charge of the external monitoring chamber. The measured temperature rise normalized to the external monitoring chamber (hereafter called "the normalized temperature rise") was as shown in Fig. 7.

The amount of radiation energy absorbed by the core was determined by taking the product of the normalized temperature rise and the effective heat capacity. The results are as shown in Fig. 8. The mean energy absorbed by the core had values of 0.798 J/μC, 0.389 J/μC, and 0.352 J/μC at 6 MV, 10 MV, and 18 MV, respectively. These values were so consistent among runs that their coefficient of variance was less than 0.15%.

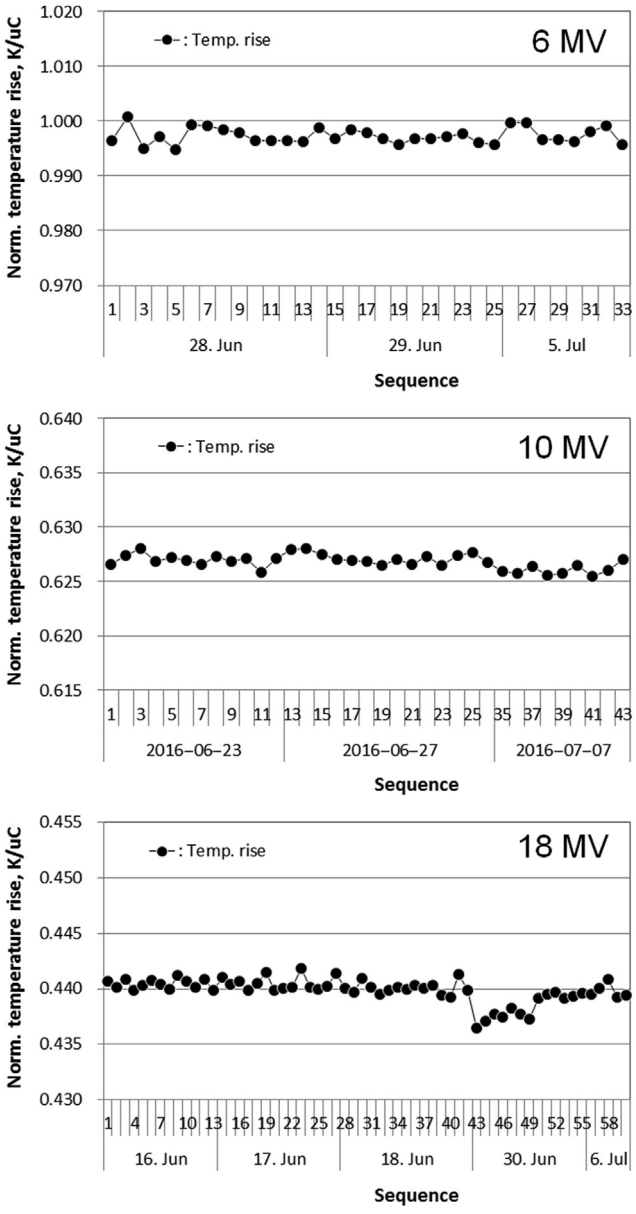

Fig. 7 – Measured temperature rise of the core by irradiation. The temperature rise was normalized to accumulated charge of the external monitoring chamber.

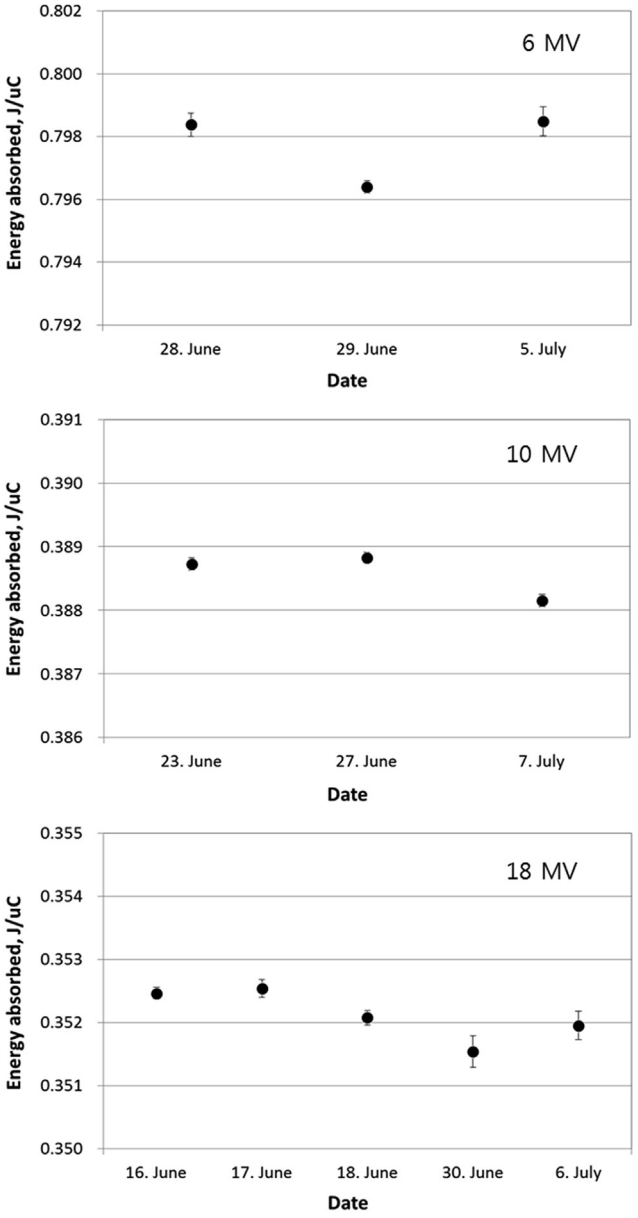

Fig. 8 – Determined energy absorbed by the core under irradiation at 800 MU. Error bars represent standard error.

4. Conclusion

In this study, a graphite calorimetry system was successfully built and showed good repeatability among repeated runs.

The calorimeter demonstrated good linearity of the core's temperature rise to electric energy of heating within a range of 6–8 mJ. The effective heat capacity of the core was determined at every run. The coefficient of variance of the effective heat capacity was approximately 0.2%; this value was mainly attributable to the poor time resolution of the electric power measurement system. Thus, it was expected that the measurement uncertainty of the effective heat capacity could be reduced if the electric power could be measured with better time resolution.

Under irradiation, the temperature of the core rose and showed a good correlation with the accumulated charge of the external monitoring chamber. Thus, the temperature rise of the core was normalized to the accumulated charge of the external monitoring chamber, and it showed better results.

The amount of radiation energy absorbed by the core was determined by taking the product of the measured effective heat capacity and the normalized temperature. All results were so consistent among runs that their coefficient of variance was less than 0.15%.

In this study, it was demonstrated how the system worked and how repeatable its working was. However, more experiments are necessary to understand the system better and to enhance the repeatability. Also, the current results are preliminary. The final purpose of the system is to determine the water absorbed dose of the X-ray beams of the accelerator. For that purpose, more studies are needed to determine parameters such as the effective mass of the core, the graphite-to-water absorbed dose conversion factor, and the nonuniformity correction of the X-ray dose distribution. Results of these kinds of studies will be reported and discussed soon.

Conflict of interest

The full description of the procedures used in this paper requires the identification of certain commercial products and their suppliers. The inclusion of such information should in no way be construed as indicating that such products or suppliers are endorsed by the authors, or are recommended by the authors, or that they are necessarily the best materials, instruments, software, or suppliers for the purposes described.

Acknowledgments

This work was supported by the Korea Research Institute of Standards and Science under the project "Establishment of Measurement Standards of Ionizing Radiations" grant 16011037. The full description of the procedures used in this paper requires the identification of certain commercial products and their suppliers. The inclusion of such information should in no way be construed as indicating that such products or suppliers are endorsed by KRISS or are recommended by KRISS or that they are necessarily the best for the purposes described.

REFERENCES

[1] S.H. Lee, Current status and future prospect of regulation for radiation safety in medicine, 2015 Winter meeting of The Korean Association for Radiation Protection, 5 Feb. 2015 (in Korean).
[2] J.S. Yang, Development of requirements for quality assurance of radiation therapy, 2015 Radiation Security Symposium, Daejeon, 9 Sep. 2015 [in Korean].
[3] KINS, Radiation Safety Information System [Internet].[cited July 2016]. Available from: http://rasis.kins.re.kr (in Korean).
[4] ICRU, Determination of absorbed dose in a patient irradiated by beams of X or gamma rays in radiotherapy procedures, ICRU Report No. 24, MD, 1976.
[5] ICRU, Dosimetry of high-energy photon beams on standards of absorbed dose to water, ICRU Report No. 64, MD, 2001.
[6] IAEA, Absorbed dose determination in external beam radiotherapy: an international code of practice for dosimetry based on standards of absorbed dose to water, TRS 398, Vienna, 2000.
[7] S.R. Domen, P.J. Lamperti, A heat-loss-compensated calorimeter: theory, design, and performance, J. Res. Natl. Stand. Sect A 78A (1974) 595–610.
[8] S.R. Domen, Advances in calorimetry for radiation dosimetry, in: K.R. Kase, B.E. Bjarngard, F.H. Attix (Eds.), The Dosimetry of Ionizing Radiation, Vol. II, Academic Press, Inc., London, 1985, pp. 245–320.
[9] J. Chavaudra, B. Chauvenet, A. Wambersie, Medicine and ionizing radiation: metrology requirements, C.R. Phys 5 (2004) 921–931.
[10] M.R. McEwen, D.T. Burns, A.J. Williams, The use of thermistors in the NPL electron-beam calorimeter, NPL Report RSA(EXT) 41, London, 1993.
[11] J.P. Seuntjens, A.R. Dusautoy, Review of calorimeter based absorbed dose to water standards, in: Proceedings of International Symposium on Standards and Codes of Practice in Medical Radiation, Vienna, Nov. 2002, IAEA-CN-96-3, Vol. 1 (2003) 37–66.
[12] J. Witzani, K.E. Duftschmid, Ch. Strachotinsky, A. Leitner, A graphite absorbed-dose calorimeter in the quasi-isothermal mode of operation, Metrologia 20 (1984) 73–79.
[13] A. Ostrowsky, J. Daures, The construction of the graphite calorimeter GR9 at LNE-LNHB, Rapoort CEA-R-6184, LNE-LNHB, 2008.
[14] J. Daures, A. Ostrowsky, B. Rapp, Small section graphite calorimeter (GR-10) at LNE-LNHB for measurements in small beams for IMRT, Metrologia 49 (2012) S174.
[15] S. Dufreneix, J.-M. Bordy, J. Daures, F. Delaunay, A. Ostrowsky, Construction of a large graphite calorimeter for measurements in small fields used in radiotherapy, 16th International Congress of Metrology, Paris, Oct. 2013, pp. 1–4.
[16] Y. Morishita, M. Kato, N. Takata, T. Kurosawa, T. Tanaka, N. Saito, A standard for absorbed dose rate to water in a 60Co field using a graphite calorimeter at the National Metrology Institute of Japan, Radiat. Prot. Dosim. 154 (2013) 331–339.
[17] S. Picard, D.T. Burns, P. Roger, Determination of the specific heat capacity of a graphite sample using absolute and differential methods, Metrologia 44 (2007) 294–302.
[18] Dupont, Kapton® HN technical Data Sheet [Internet].[cited 1 August 2016]. Available from: http://www2.dupont.com/Kapton/en_US/assets/downloads/pdf/HN_datasheet.pdf.
[19] J.S. Steinhart, S.R. Hart, Calibration curves for thermistors, Deep-Sea Res. Oceanogr. Abstr. 15 (1968) 497–503.